Case Study

Revisiting Tavenas (1971): Tests on Piles in Sand

Bengt H. Fellenius[1]*

Abstract: Tavenas (1971) performed a sequence of static loading tests on telltale-instrumented precast concrete piles and H-piles driven in compact fine to medium sand. The first test of the sequence started at 6 m depth and continued with five more tests after driving each pile an additional 3-m length at a time. The instrumentation was intended for use in separating shaft and toe responses. In particular for the precast pile, the test results implied a strain-hardening response, which detailed back-analysis showed to be due to gradually increasing overestimation of the applied load. The original analysis and interpretation of the test records ostensibly confirmed the existence of a "critical depth". However, when correlating the analysis to potential presence of residual force and adjusting the distribution of overburden stress to the fact that the piles had been driven in an excavation, the test data instead confirmed that, instead, all pile response followed the distribution of effective overburden stress.

Keywords: precast concrete pile, H-pile, telltales, static loading tests, back-analysis, load-movement

Introduction

Tavenas (1971) reported a case history of a series of full-scale head-down static loading tests in Quebec, Canada, performed in 1968 to compare the response of a 12-inch, hexagonal, precast concrete pile and a 12-inch H-pile, both telltale-instrumented, driven into sand for use in the design of foundations for a long retaining wall. The testing programme comprised interrupting the pile driving at every about 3 m depth to perform a static loading test aiming to establish distribution of shaft and toe resistance. The case and the paper have special interest to me because I was at the time working for the contractor, A. Johnson Co., Montreal that performed the tests. I attended them all and collaborated with Dr. Tavenas on the analysis of the results. I also have the benefit of still having the original test records.

Soil Profile

The original site profile was composed of a 7.4 m thick layer of old fill underlain by a 16 m thick layer of poorly graded compact fine-to-medium sand. At about 23 m depth, an about 0.6 m thick layer of very dense gravel was found followed by stiff clay extending to large depth. To reproduce the working conditions for the finished structure, a 10 by 30 m trench was excavated down to the surface of the sand and partially backfilled with 5 m of crushed stone (sand and gravel) dumped under water and left uncompacted. Figure 1 shows a vertical section of the site showing trench geometry, soil profile, and length of piles for each test for the so-prepared test site. Figure 2 comprises the grain size boundaries of the sand and shows that the sand contained 80% of fine sand with a trace of silt. Figure 3 shows distribution of N-indices from a borehole at the test location drilled after the site had been excavated and back-filled. The split-spoon samples showed the sand to have dry and saturated total densities of about 1,600 kg/m^3 and 2,000 kg/m^3, respectively

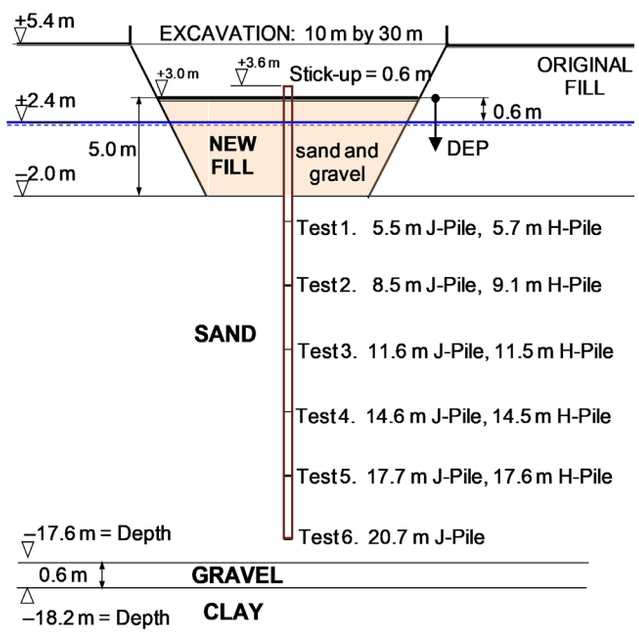


Figure 1. Vertical section of the test site

[1] Consulting Engineer, 2475 Rothesay Ave, Sidney, BC, Canada, V8L 2B9
* Corresponding author, e-mail: bengt@fellenius.net

© 2025 Deep Foundations Institute,
Print ISSN: 1937-5247 Online ISSN: 1937-5255
Published by Deep Foundations Institute
Received 31 May 2023; received in revised form 7 September 2023; accepted 15 October 2023
Paper DOI: https://doi.org/10.37308/DFIJnl.20230531.282

vol19no1fellenius282.indd 1 09/07/25 5:03 PM

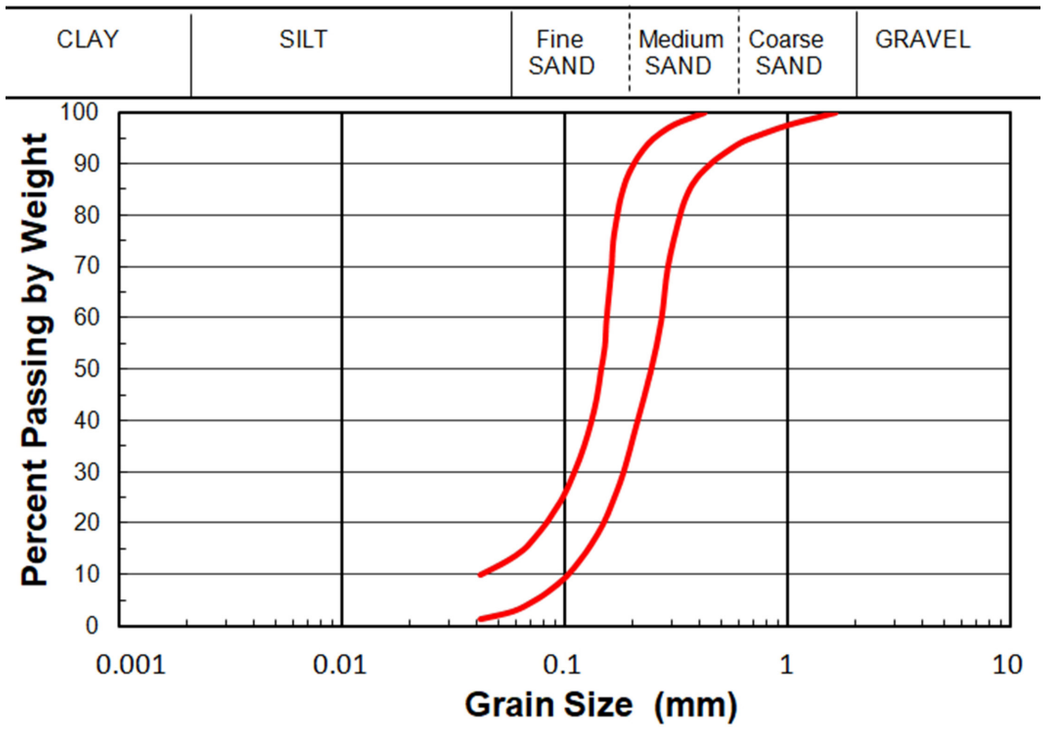


Figure 2. Grain size distribution of the natural sand

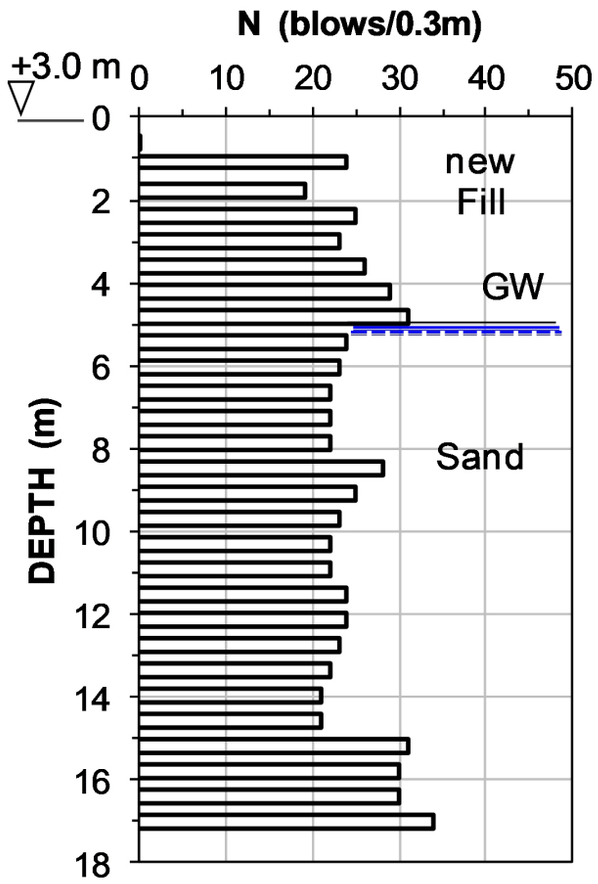


Figure 3. N-indices distribution

Piles and Instrumentation

The piled foundation for the project was to support 343 kN/pile unfactored load and the pile alternatives considered were a hexagonal precast concrete pile, Herkules H800, here called the J-pile, and an H-pile, 12BP74. The nominal pile cross section and surface area of the J-pile were 800 cm^2 and 1.05 m^2/m, respectively. For the H-pile, the nominal areas were 141 cm^2 and 1.80 m^2/m, respectively. The area of a square circumscribing the H-pile was 1.22 m^2/m. The J-pile was cast with a 38 mm (ID) steel center tube. The telltale outer guide pipes added 5 cm^2 to the H-pile cross section area and 0.05 m^2/m to the surface area. Both piles were made up of segments delivered to the site in one 6 m and five 3 m lengths. They were driven to incremental embedments depths of about 6, 9, 12, 15, 18, and 21 m using a 3-tonne drop hammer. The 6-m segments were driven first.

The piles were instrumented with telltale rods to measure axial compression of the full pile length and between the pile head and a depth above the pile toe. For the J-pile, the telltales comprised an oil-filled 19-mm outer pipe and a 9.5 mm rod placed inside the pipe, both inserted in the pile center tube after driving. The inner rod extended to the pile toe. The 19 mm pipe was equipped with a device for locking onto the inside of the center tube at a designed depth above the pile toe, serving as the shorter telltale (Broms and Hellman 1968). The telltales were removed after each static test and reinserted for the next test.

For the H-pile, two 6 mm telltale rods were inserted after driving in a guide pipe consisting of an oil-filled 19 mm tube welded to the pile flanges at intervals with special coupling of

© Deep Foundations Institute

vol19no1fellenius282.indd 2 09/07/25 5:03 PM



Figure 4. Photo of test arrangement for the precast pile (photo by B.H. Fellenius)

the guide pipes between pile segments (Bozozuk and Jarrett 1967).

The telltale ends were at the pile toe and at a point about 6 m above the pile toe. Thus, the compression of the pile for all applied loads was obtained over the full length, an upper length, and a lower length by differentiation. The compression records were converted to average strain by division with the respective telltale length and length difference (lower length value). The steel-H-pile was Grade B with, therefore, a 240 GPa E-modulus. Compression tests on two one metre long sections cut from the precast pile (with center tube) and stored under water showed an average E-modulus of 27 GPa. These values were combined with the mentioned total cross-sectional areas of the two piles to correlate to pile axial EA-parameters of 3.40 and 2.16 GN, respectively.

The first static loading test for each pile was carried out after driving the 6 m pile segment. Next, a 3-m segment was added using, for the J-pile, a mechanical splice cast with the pile with arrangement for the center tube and, for the H-pile, by welding the ends of the respective H-sections together and connecting the guide-pipes. After the end of the driving to each new test depth, a 12-hour wait was imposed before the next static test was commenced.

The static loading tests consisted of applying 111-kN (25-kip) equal load increments of load, maintaining each load level for 60 minutes until continuing pile-head movements indicated that ultimate resistance had been reached. Loads were determined from pressure in the hydraulic pump fluid. The test schedule included no unloading-reloading events. No separate load cell was employed

For unknown reasons, the sixth test on the H-pile gave inconsistent data for both applied load and telltale movements. Those records are therefore, excluded. The fact that the piles were driven in an excavation excavation, which affected the overburden stress distribution, as indicated by a Boussinesq stress calculation (requiring computer calculation, which was not available in 1968 and, therefore, this adjustment of the effective overburden stress was then omitted. It is however included in the here presented analysis results).

Figure 4 shows a photo of the test setup for the precast concrete pile with reaction piles driven 2.0 m away from the test pile. Two jacks were used to provide the telltale rods with obstruction-free exit from the center pipe. The arrangement for the H-pile was with one jack, only, as the telltale measurements were against the side of the pile. The canvas was used to shield the measuring beam from sunlight and crew from rain.

Test Results

Load-movement

Figure 5 shows the pile-head load-movement curves from Tests J-pile and H-pile. The red dots are the ultimate resistances as "eyeballed" by Tavenas (1971) from the curves. It is worth noticing that they are close to what would be found by applying the Davisson Offset method (Davisson 1972). The black plus signs for Tests J4 – J6 and Tests H4 – H5 indicate actually applied loads, close to Tavenas' values, here chosen as the target force distribution for fitting an effective stress analysis to the resulting distributions of axial force after converting compressions to strain. The calculations were performed using the UniPile software (www.UnisoftGS.com).

Compression, strain, and stiffness

The telltales in each of the two test piles gave measurements of the compression of the pile along the telltale lengths—the full length and the upper pile length. The difference between

© Deep Foundations Institute

vol19no1fellenius282.indd 3 09/07/25 5:03 PM

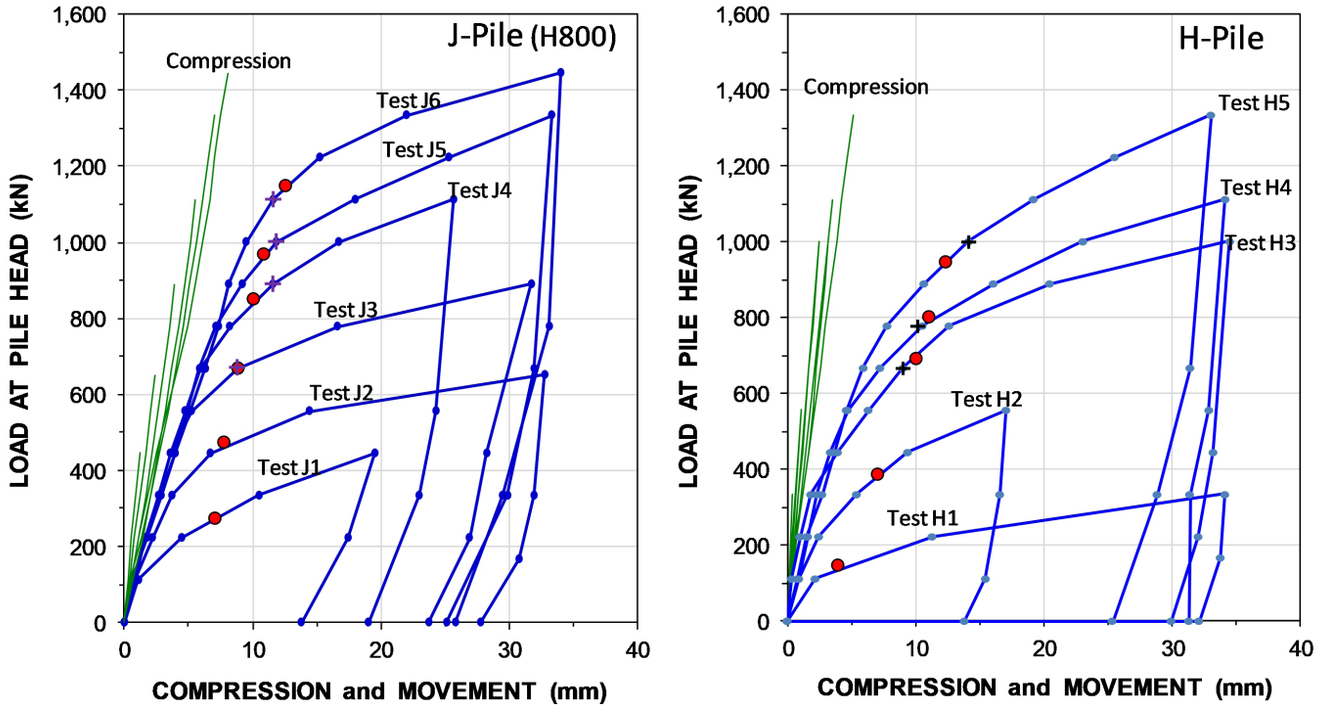


Figure 5. Pile-head and pile-compression load-movement curves for the two tests series

the two telltales gave the compression along the lower, about 6 m length of the pile. Dividing the values by the telltale lengths provided the average strain along each respective telltale length. The axial loads represented by the values of average strain were calculated by multiplying each strain value with the mentioned axial EA-parameter $(EA)_J$ = 2.16 and $(EA)_H$ = 3.40 GN, for the J-pile and H-pile, respectively).

The mentioned EA-parameters have large credibility. For the steel, this is obvious. For the concrete pile, the use of compressing a specimen of the actual pile under controlled laboratory condition avoided the obvious uncertainty estimating the E-modulus from cylinder strength. Alternatively, the axial stiffness, EA/L, could have been used by applying the tangent EA-parameter determined from the slope of the applied load vs. strain (Fellenius 1989; 2022). However, this would not be applicable to applicable to strain determined as an average over a length, only to strain records from a strain-gage placed near the pile head. Nevertheless, Figure 6 shows the tangent EA-parameter calculated from the test data for the upper and full length telltales. The lower length EA-parameters are not shown because they are not useful because of the differentiation involved—the difference between the two telltale records combines the error of each and the error in evaluated EA-parameter is, therefore, considerable exacerbated. The scatter displayed in the figure is considerable, but no more than would be expected from telltale measurements.

In Figure 6, the initial portion of the curves indicates a reducing EA-parameter, followed by a mid-portion with approximately level values, then, changing to increasing trend for the end portions, in particular for the J-pile. The first portion is because the increasing shaft resistance reduces the average force along the telltale length. The end portion is typical of a soil with strain-hardening response—or indicates increasing error in the values of applied load. The mid-portion "leveled out" value would then be the actual pile EA-parameter. However, in a strain-hardening soil, it too would be somewhat larger than the true value.

To smooth over the scatter of the tangent EA vs. strain diagrams (c.f., Figure 6), the EA can be estimated from the slopes of applied load vs. strain as shown in Figure 7. The slope of the curves once the shaft resistance has been mobilized, and provided that the soil response is plastic, can be considered as approximately equal to the pile axial EA-parameter. The red lines show the slopes equal to the $(EA)_J$ and $(EA)_H$.

The difference between the laboratory determined EA-parameters and those suggested by Figures 6 and 7 is larger than what a moderate strain-hardening soil response would provide. As stated below, the reason is likely that the applied load is overestimated, and this to an increasing degree as the test progressed.

The overestimation is because the applied load was determined from the pressure in the hydraulic fluid, which is affected by the force to overcome the friction in the expanding jack. This error can range between a few percentage points to be 25 % or more of the true load, but is usually about 10 % (Fellenius 1984; 2023). The upward curving of the lines from the concrete pile could be due to strain-hardening or to increased friction affecting the telltale records. As the lines from the H-pile show only minor such increasing trend, the upward curving of the Pile-J lines is likely not due to strain-hardening, but to friction

© Deep Foundations Institute

vol19no1fellenius282.indd 4 09/07/25 5:03 PM

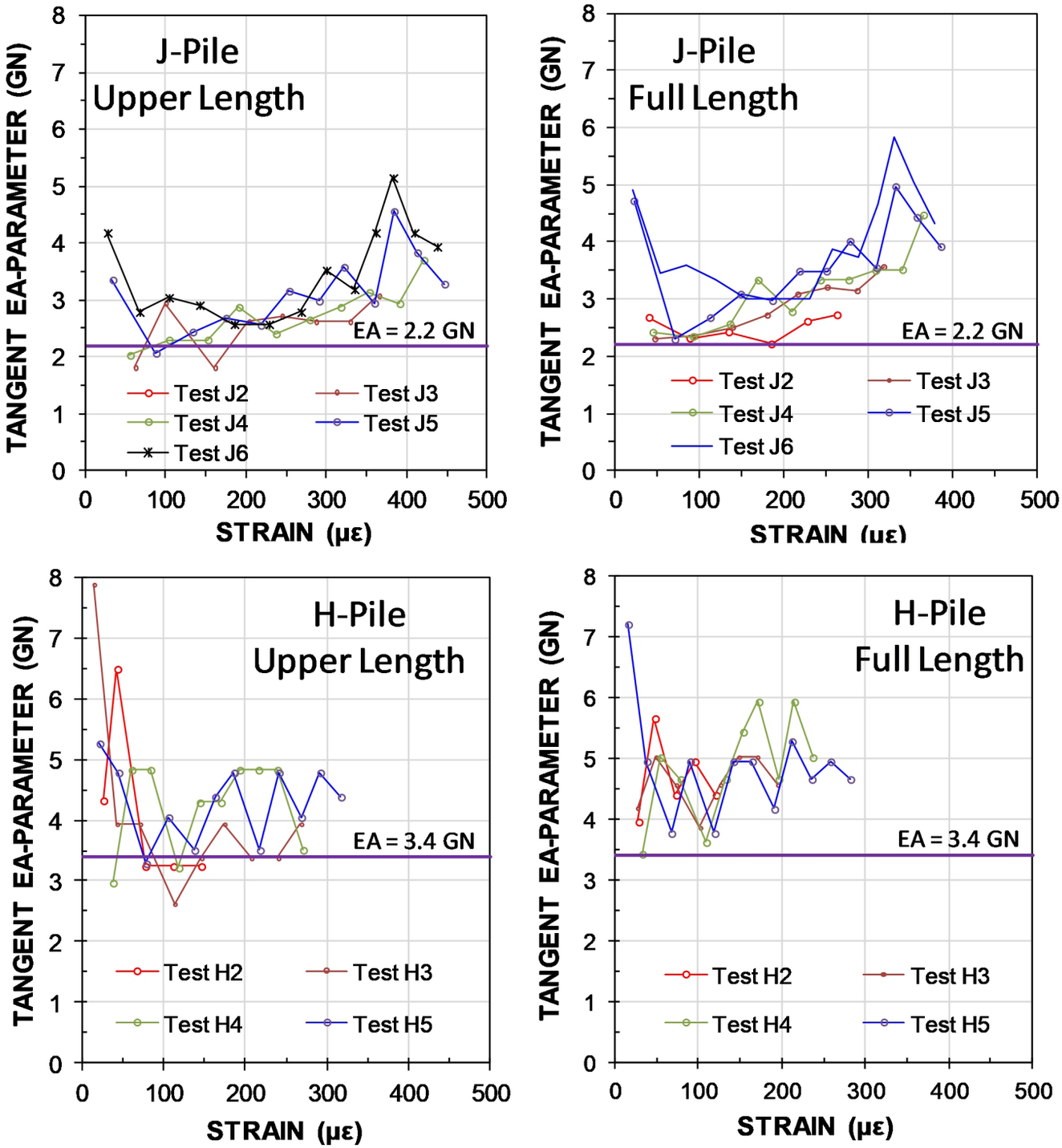


Figure 6. Tangent EA-parameter over upper and lower lengths for the two tests series

along the telltale rod. Neither is likely due to any change of axial stiffness, because if the E-modulus of concrete would have changed with the increase of stress, the axial stiffness would have reduced, i.e., the trend would then have indicated a curving-down of the lines. In summary, both tests were considered affected by overestimation of the applied load. In addition, the strain records of the precast pile were probably affected by gradually increased error in the applied load (overestimation error in the jack pressure), which is more likely to occur in a two-jack system employed for the J-test for the later test loads as the jack piston rises out of the jack cylinder (c.f., Figure 2).

Distribution of axial force

Determining the average axial force from the strain data is independent of any error in the applied load. Figure 8 shows

© Deep Foundations Institute

vol19no1fellenius282.indd 5 09/07/25 5:03 PM

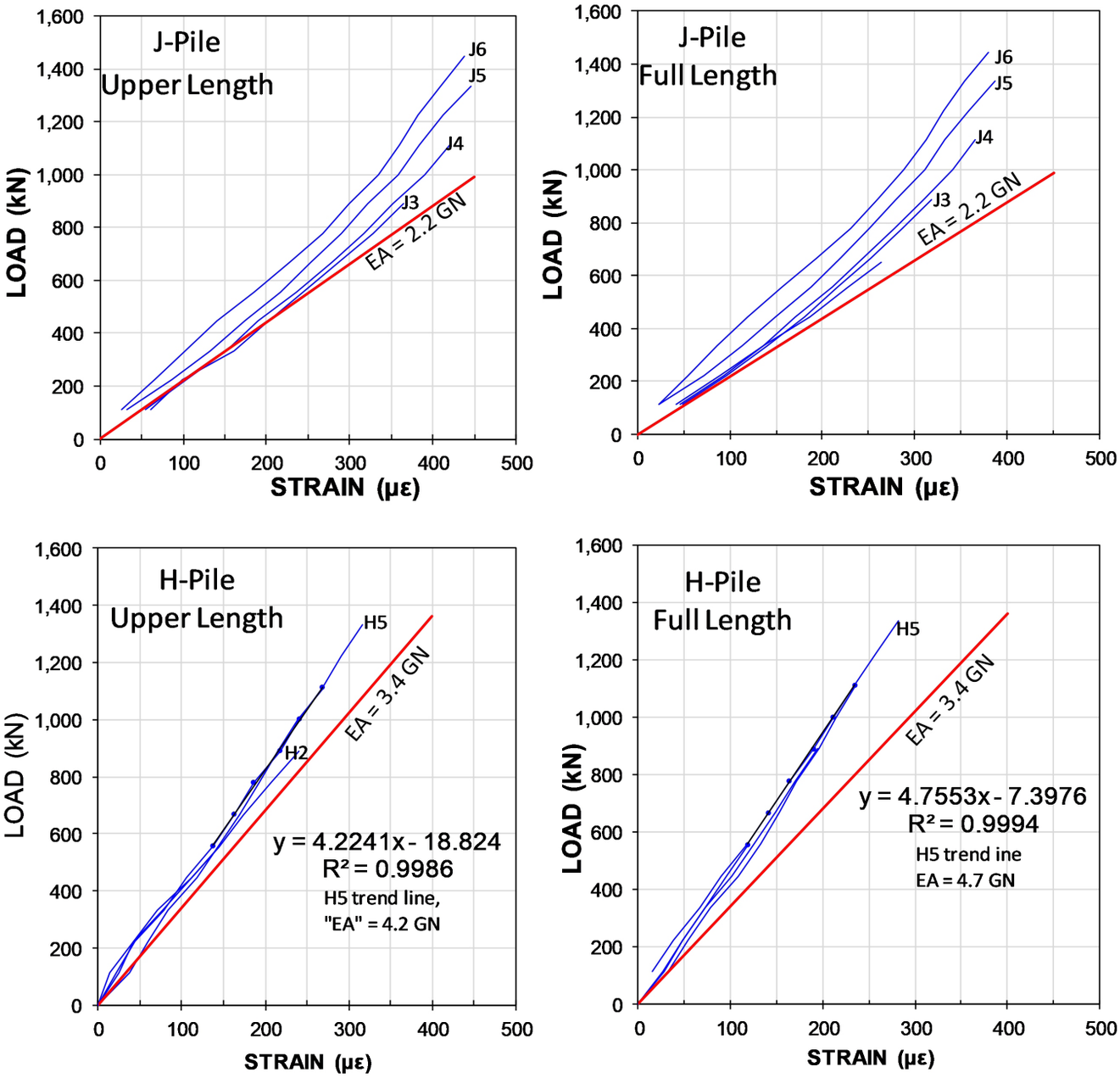


Figure 7. Applied load vs. strain

the distributions of strain-determined force from Tests J4 - J6 and H4 - H5, using the axial EA-parameters, $(EA)_J$ = 2.16 and $(EA)_H$ = 3.40 GN, respectively. The distributions connect the applied load to the axial forces calculated from the strain and plotted at mid-point of each telltale length, one value for each telltale and a third for the distance between the end of the upper telltale and the pile toe, from where the line is extrapolated to the pile toe. The red dots indicate the ultimate resistances chosen by Tavenas (1971) and the red lines are the distributions selected as target for my analysis. The latter were selected as being for an applied load that appeared to have just about engaged all elements of the pile including the pile toe. The close agreement between the two selections is no coincidence.

The force distributions in Figure 8 are almost linear. This would suggest that the mobilized shaft resistance is constant and not proportional to the effective overburden stress. Tavenas (1971) reported that for Piles J5 and H5, the ultimate shaft resistance in the sand below the backfill was plastic and about 25 kPa and was reached after 5 mm movement and that about the same values were found in all Pile J tests, but were about 15 kPa for Tests H2 - H4 and about 25 kPa for Test H5. The H-pile shaft area was taken as that of the circumscribed square.

Tavenas (1971) also reported that also the toe resistance was constant with depth and that the toe resistance, as extrapolated from the force distribution, increased steeply over the

© Deep Foundations Institute

vol19no1fellenius282.indd 6 09/07/25 5:03 PM

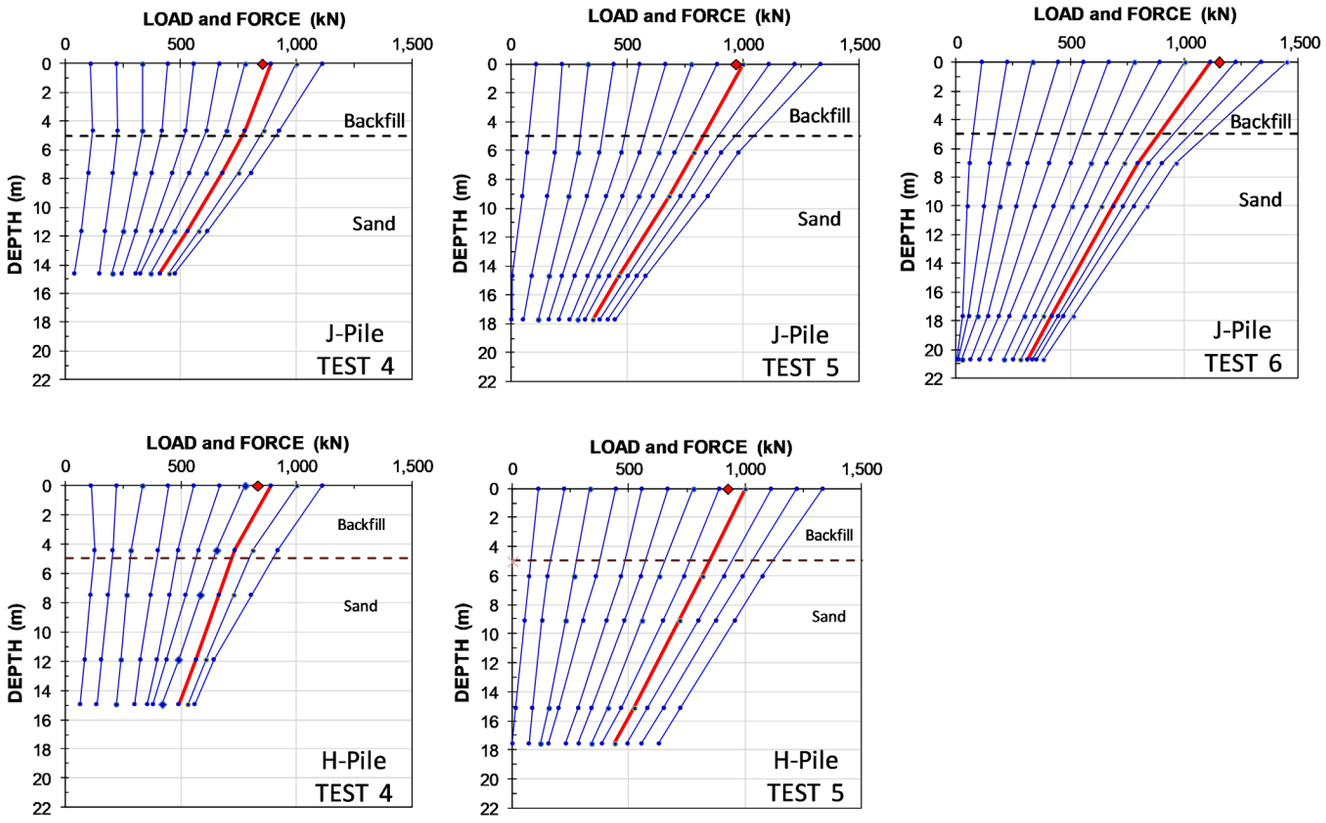


Figure 8. Distributions of axial force

first about 35 mm beyond which a large increase of toe movement was observed. This value was defined as the ultimate toe resistance and was about 4.3 - 4.6 MPa for Tests J3 - J6 and about 3.6 - 4.1 MPa for Test H3 - H5. The toe area was defined as that of the circumscribed square.

A few papers, e.g., Vesic (1964; 1970) and Kerisel (1971), have indicated that it is to be expected that both ultimate shaft and toe resistances should show to be constant below a specific depth and proposed a "critical depth" theory to explain it. At the time, both Dr. Tavenas and myself drove the conclusion expressed by Tavenas (1971): "*The results of loading tests ... confirm the observations made by ... Vesic (1964). A ... critical depth was defined at a depth to diameter ratio, D/b, of 23, below which the ultimate toe shaft and resistances are perfectly constant*".

Now, 50 years later, we do know that ultimate resistance is a matter of definition and that pile toe resistance based on load-movement response does not exhibit an ultimate resistance by any definition. Moreover, we know that the appearance of a "critical depth" and appearance of constant shaft and toe resistance is false and caused by the presence of residual force.

Figure 8 combines the applied load with the forces determined from the telltale strain records. The applied load and it is clearly overestimated to some degree, as addressed in the foregoing and below. The slope of the distribution curves within the backfill should be steeper than shown in the diagrams and the curves rising from the strain-gage calculated forces should connect to a smaller applied load than shown.

The straight-line appearance of the force-distributions are the effect of the presence of residual force. After a few trial-and-error analyses including a correction for the jack overestimation of the applied load (effected by adjusting the assumed shaft resistance in the back-fill), I found that the test records could be simulated by a "true" distribution based on an effective stress calculation including the excavation effect.

Figure 9 shows the so-determined "true" distributions (red curves) for Tests J5 and H5, the target distributions. Subtracting these distributions from the measured (the curve with circular symbols) gave the distributions of residual force (light blue curve). The process is not arbitrary. The basic assumption is that, first, the shaft resistance is the same in the negative and positive shear directions and, second, that the shaft resistance has reached a plastic state for the analyzed distribution. Therefore, the "true" shaft resistance (the green curves starting at zero at the ground surface and progressing to the toe) cannot be smaller than half the apparent shaft resistance. This means, that the "true" distribution (red curve) cannot plot steeper than (cannot cross) the yellow curve with plus symbols. Moreover, the "true" toe resistance cannot be smaller than the "false" toe resistance. Third, the simulated residual curve (light blue curve nearest the ordinate)

© Deep Foundations Institute

vol19no1fellenius282.indd 7 09/07/25 5:03 PM

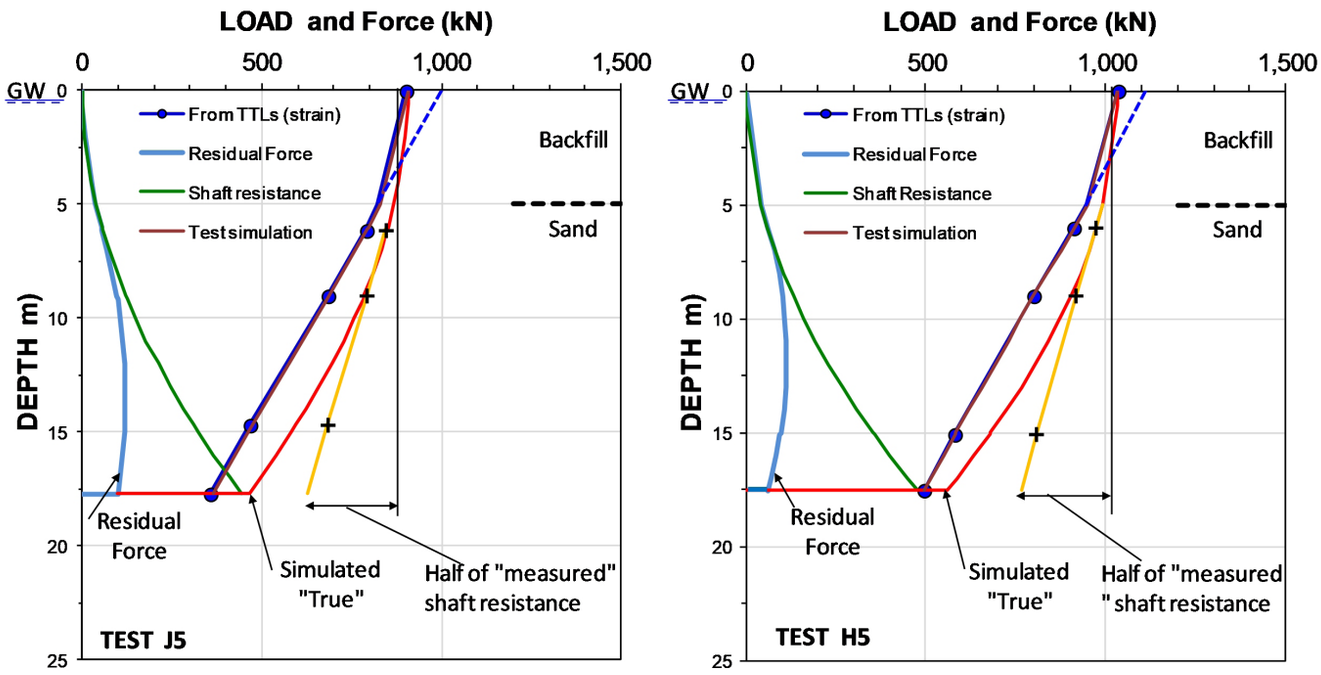


Figure 9. Load-and force movements

cannot rise from the pile toe at a slope flatter than the simulated "true" curve, nor be flatter anywhere else. The "true" distribution is then fitted in between a reasonably smooth rise from an assumed toe resistance to the load at the pile head. The simulated "true" distribution curve can take any shape between the pile head and pile toe, but, to repeat, it must not cut across the "half of measured distribution" (the curve with plus symbols). For the subject case, because of the uniformity of the soil, the same ß-coefficient is assigned throughout the pile length. This decided the distributions of "true" force and residual force, the red and light blue curves shown for the two piles. The difference between the red curve and the blue dashed line below the pile head indicates the error in the applied load (the jack error). The back-analysis and simulations were carried out using the UniPile software (www.UniSoftGS.com).

For both piles, to simulate the target distribution, the unit shaft resistance was calculated applying a beta-coefficient of 0.20 and a unit toe resistance of 5,800 kPa. The circumference areas of the J-pile and the H-pile were 1.05 m^2/m 1.23 m^2/m, respectively. For the H-pile, both the shaft shear and the toe stress were assumed to act on the equivalent square cross section of the pile. The pile-toe movements were about equal, 12 and 15 mm, respectively.

Similar analysis procedure applied to Tests 4 and 6 gave essentially the same results in regard to ß-coefficient, toe resistance, and residual force.

Conclusions

The test records are of unusually good quality for its time enabling re-analysis of the test records. The following conclusions resulted from the new back-analysis

(1) It is interesting that the back-calculated shaft and toe resistances were about equal for the two types of test piles, despite their obvious differences of shape and material. N.B., the H-pile was analyzed with the shaft resistance acting around the square circumference as opposed to the H-section.
(2) When the concept of residual force was considered, the original conclusions in regard to "critical depth" were shown invalid and that the response of the pile shaft to an applied load is proportional to the overburden effective stress along its full length.
(3) The residual force left in the pile after driving was fully mobilized along the upper about half length of the piles.
(4) The tests show that the use of a separate load cell to measure the applied load is essential for minimizing errors in the back-analysis.
(5) The repeated driving did not appear to have caused the beta-coefficient along the previously driven depths to differ from that along the added 3 m length.

Acknowledgement

Francois Tavenas was well aware of the understanding brought forward in the late 1970s of the effect of residual force. In fact, in around Year 2000, we agreed that that test records warranted a reanalysis and decided that we should revisit his 1971 paper. Unfortunately, we both got busy and Tavenas' untimely passing in 2004 shelved the effort. However, I recently saw a paper citing Tavenas' 1971 paper in support of the "critical depth", and I thought I would go on record that we both through the years kept learning and had our thoughts evolve.

© Deep Foundations Institute

vol19no1fellenius282.indd 8 09/07/25 5:03 PM

References

Bozozuk, M. and Jarrett, P.M. (1967). Instrumentation for negative skin friction studies on long piles in marine clay on the Autoroute du Quebec. *Proceedings of the International Bridge Tunnel and Turnpike Association*, 1967, pp. 44-64.

Broms, B.B., and Hellman, L. (1968). End-bearing and skin-friction resistance of piles. *Journal Soil Mechanics and Foundations*, ASCE, Vol. 94, No. SM2. 421-429.

Davisson, M.T. (1972). High capacity piles. *Proc. of Lecture Series on Innovations in Foundation Construction*, ASCE Illinois Section, Chicago, March 22, pp. 81-112.

Fellenius, B.H. (1984). Ignorance is bliss—And that is why we sleep so well. Geotechnical News, Canadian Geotechnical Society and United States National Society for Soil Mechanics and Foundation Engineering, Vol.2, No.4, pp. 14-15.

Fellenius, B.H. (1989). Tangent modulus of piles determined from strain data. *ASCE, Geotechnical Engrg. Div., 1989 Found. Congress*, F. H. Kulhawy, ed., 1, 500–510.

Fellenius, B.H. (2025). Basics of foundation design. Electronic Edition, www.Fellenius.net, 572 p.

Goudreault, P.A. and Fellenius, B.H. (2014). UniSoft Geotechnical Software, www.UniSoftLtd.com

Kerisel, J. (1961). Fondations profondes en milieusableux. *Proceedings of the Fifth International Conference on Soil Mechanics and Foundation Engineering ICSMFE*, Paris, July 17-21, Vol. 2, pp. 73-83.

Tavenas, F.A. (1971). Load test results on friction piles in sand. *Canadian Geotechnical Journal* 8(7) 7-22. https://doi.org/10.1139/t71-002

Vesic, A.S. (1964). Investigations of bearing capacity of piles in sand. *Proc. of North American Conference on Deep Foundations*, Mexico City, December 1964. pp. 197-224.

Vesic, A.S., (1970). Test on instrumented piles, Ogeechee River site. *ASCE Journal of the Soil Mechanics and Foundations Division,* Vol 96, Issue 2, 561-584. https://doi.org/10.1061/JSFEAQ.0001404

DFI Journal Underwriters

NUCOR® SKYLINE

MALCOLM Look to the Blue

Tectonic PRACTICAL SOLUTIONS. EXCEPTIONAL SERVICE.

RBM

INTERNATIONAL CONSTRUCTION EQUIPMENT ICE 888-ICE-USA1 WWW.ICEUSA.COM

Pile Dynamics, Inc.

UES™

© Deep Foundations Institute

vol19no1fellenius282.indd 9 09/07/25 5:03 PM